CHARACTERIZATION OF MARE EJECTA EMPLACEMENT DIVERSITY: INSIGHTS FROM MINI-RF. A. M. Stickle[1], G. W. Patterson[1], D. B. J. Bussey[1], J. T. S. Cahill[1], and the Mini-RF Team, [1]Johns Hopkins University Applied Physics Laboratory, Laurel, MD (angela.stickle@jhuapl.edu).

Introduction: We use circular polarization ratio (CPR) profiles to investigate properties of lunar crater ejecta in mare terrains. Within 10 craters studied here, significant diversity is observed in average CPR profiles as a function of crater radius. This diversity may be a function of crater size or may be an expression of subsurface layering. These data suggest that CPR information of lunar craters can isolate the surface expressions of discrete layering within mare terrain.

Background: The Miniature Radio Frequency (Mini-RF) instrument flown on NASA's Lunar Reconnaissance Orbiter (LRO) is a Synthetic Aperture Radar (SAR) with a hybrid dual-polarimetric architecture. I.e., the radar transmits a circularly polarized signal, and receives orthogonal linear polarizations and their relative phase [1]. The returned information can be represented using the classical Stokes parameters (S_1, S_2, S_3, S_4) [2], which can be used to derive a variety of useful products to characterize the radar scattering properties of the lunar surface. CPR is commonly used in analyses of planetary radar data [3-4] and is given by: CPR = $(S_1-S_4)/(S_1+S_4)$. It is a representation of surface roughness on the order of the radar wavelength (e.g., boulders).

We examined the radar scattering properties of the ejecta blankets for 10 young, fresh, mare craters (Table 1) with diameters ranging from 7–55 km. Average profiles of the Stokes parameters (S_1 and S_4), and CPR were calculated as a function of radius for each crater, beginning at the crater rim and extending outward for 100–200 km.

Table 1. Summary of craters examined in this study

Crater	D [km]	Latitude	Longitude
Harpalus E	7	52.7	-50.8
Louiville D	7	46.9	-52.1
Bessarion	10	14.9	-37.3
Gambart A	12	1.0	-18.7
Dionysius	18	2.8	17.3
Euler	27	23.3	-29.2
Kepler	31	8.1	-38.0
Petavius B	33	-19.9	57.1
Harpalus	39	52.6	-43.4
Aristillus	55	33.9	1.2

Observations and Analysis: Comparing scattering properties as a function of radius reveals information about ejecta emplacement in mare craters. Some commonalities in the scattering profiles are observed for all crater diameters: higher CPR values occur near the crater rim, which decay with radial distance outward. Figure 1 shows profiles of CPR as a function of distance from the crater rim for five mare craters. In this context, these craters have similar CPR profiles. There is a progression with crater diameter: larger craters have a higher CPR than smaller craters (with the exception of Harpalus E) and the overall shapes of the profiles are similar.

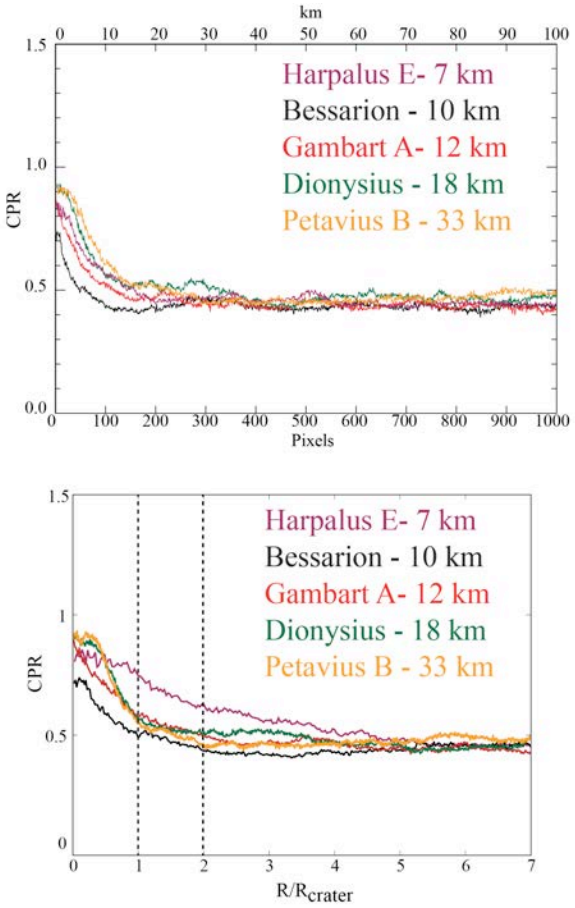

Figure 1. (top) Average CPR as a function of distance from the crater rim. (bottom) Average CPR profiles as a function of crater radius outward from the crater rim,

When distance from the crater rim is normalized to crater radius (Fig 1. bottom), however, these trends are not as obvious. The overall size progression is still apparent and larger craters have higher CPR near the rim. However, the profile shapes are no longer similar across the size range, and the high CPR "shelf" near the rim is more pronounced, with a region of high CPR extending out to ~0.5 R_c before the signal transitions to

the lunar background value. Gambart A and Harpalus E, however, do not follow this trend. A laterally extensive region of high CPR is not observed at Gambart A, where CPR begins to decrease immediately outside the crater. These observations are contrary to what would be expected from optical images, where there is a large, optically bright ejecta blanket around the crater. In contrast, the CPR is high near the rim of Harpalus E and the surface remains rough (with moderate to high CPR values) out to several crater radii from the rim, unlike other are craters. It is possible that age may account for these differences in profile shape. Although all five craters are Copernican, perhaps crater degradation is more apparent in the roughness of the surface than in optical images.

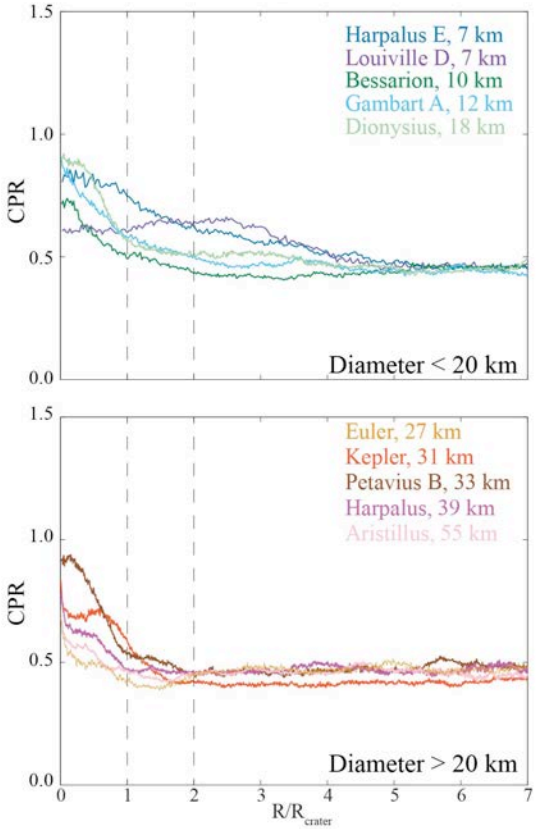

Figure 2. Profiles of average CPR as a function of normalized distance from the crater rim. (top) Mare craters with diameters less than 20 km. (bottom) Mare craters with diameters > 20 km.

Figure 2 compares CPR profiles to crater size. With the exception of Petavius B, all the mare craters > 20 km have similar scattering profiles, though different in magnitude. The CPR drops rapidly near the crater rim, but then remains constant for a short distance before dropping again to the lunar background level. These shelves neither begin nor end at the same relative radius from the crater rim. We hypothesize that these results reflect radar observations of subsurface layering. The mechanical property differences between layers could result in more blocks on the order of the radar wavelength to be emplaced on the surface, causing a bench in the CPR profile. This hypothesis agrees with preliminary M^3 observations [5] that show differing compositions of material being ejected in these craters.

These observations reveal that CPR profiles observed adjacent to craters (e.g., Kepler crater) may provide insight regarding subsurface layering in mare regions. Hörz *et al.* [6] estimate that the dominant source depth for primary ejecta within the continuous ejecta blanket is <0.01 times the crater diameter. To a first order, the depth from which material in the continuous ejecta blanket (within approximately 1 crater radius from the rim [7]) is excavated at Kepler crater would then be approximately 300 m, consistent with the approximate depth of the layering observed in LROC NAC images (Fig. 3). Thus the CPR profile from Kepler crater may be revealing a discrete subsurface layer that was emplaced at the surface during the impact process.

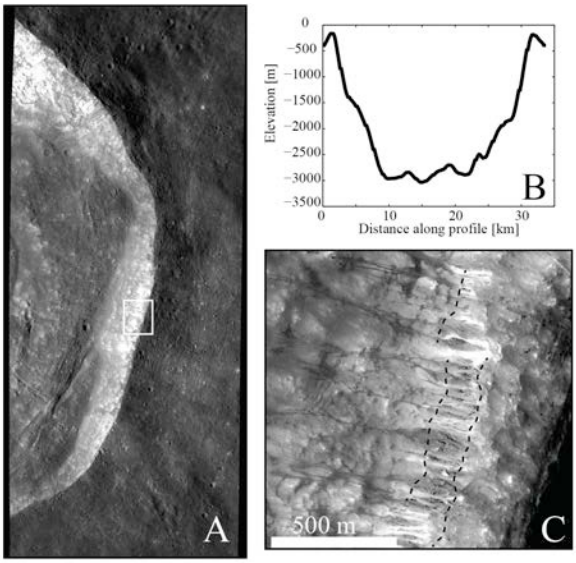

Figure 3. A) LROC NAC mosaic of Kepler Crater (31 km); B) topographic profile of Kepler, across the middle of the crater, E to W; C) NAC image of layering in the wall of Kepler crater, indicated by white box in A. Dotted lines show approximate edges of subsurface layers observed behind landslides.

References: [1] Raney, R. K. et al. (2011), *Proc. of the IEEE*, 99, 808-823; [2] Stokes (1852), Trans. of the Cambridge Phil. Soc. 9, 399; [3] Campbell et al. (2010), *Icarus*, 208, 565-573; [4] Carter et al. (2012), JGR, 117, E00H09; [5] R. Klima, personal communication; [6] Hörz, F. et al. (1983) *Rev. Geophys. and Space. Phys.*, 21, 1667-1725; [7] Moore et al. 1974, *Proc. 5th LPSC,* 71-100.